Science of the Total Environment 794 (2021) 148589

Contents lists available at ScienceDirect

Science of the Total Environment

journal homepage: www.elsevier.com/locate/scitotenv

Diurnal variability in the spectral characteristics and sources of water-soluble brown carbon aerosols over Delhi

Neeraj Rastogi [a,*], Rangu Satish [a], Atinderpal Singh [a,1], Varun Kumar [b], Navaneeth Thamban [c], Vipul Lalchandani [c], Ashutosh Shukla [c], Pawan Vats [d], S.N. Tripathi [c], Dilip Ganguly [d], Jay Slowik [b], Andre S.H. Prevot [b]

[a] Geosciences Division, Physical Research Laboratory, Ahmedabad 380009, India
[b] Laboratory of Atmospheric Chemistry, Paul Scherrer Institute, Villigen 5232, Switzerland
[c] Department of Civil Engineering and Centre for Environmental Science and Engineering, Indian Institute of Technology Kanpur, Kanpur 208016, India
[d] Centre for Atmospheric Sciences, Indian Institute of Technology Delhi, New Delhi 110016, India

HIGHLIGHTS

- Diurnal characteristics of brown carbon (BrC) spectra are investigated.
- Multiple events with unusually high absorption at 490 nm are observed.
- Positive matrix factorization analysis on BrC spectra revealed four factors.
- Biomass burning derived BrC is most absorbing among all sources.

GRAPHICAL ABSTRACT

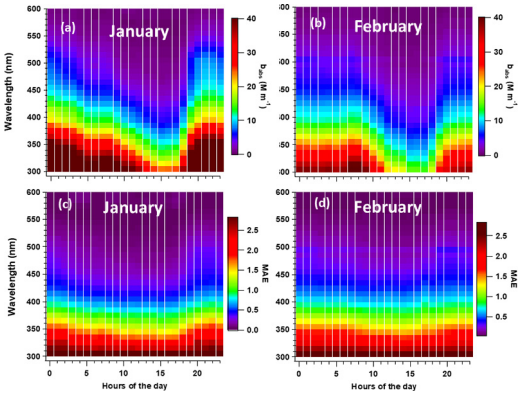

ARTICLE INFO

Article history:
Received 24 February 2021
Received in revised form 1 June 2021
Accepted 17 June 2021
Available online 25 June 2021

Editor: Pingqing Fu

Keywords:
Light absorbing species
Mass absorption efficiency
Chromophores
Megacity
Indo-Gangetic Plain

ABSTRACT

It is well established that light-absorbing organic aerosols (commonly known as brown carbon, BrC) impact climate. However, uncertainties remain as their contributions to absorption at different wavelengths are often ignored in climate models. Further, BrC exhibits differences in absorption at different wavelengths due to the variable composition including varying sources and meteorological conditions. However, diurnal variability in the spectral characteristics of water-soluble BrC (hereafter BrC) is not yet reported. This study presents unique measurement hitherto lacking in the literature. Online measurements of BrC were performed using an assembled system including a particle-into-liquid sampler, portable UV–Visible spectrophotometer with liquid waveguid capillary cell, and total carbon analyzer (PILS-LWCC-TOC). This system measured the absorption of ambient aerosol extracts at the wavelengths ranging from 300 to 600 nm with 2 min integration time and water-soluble organic carbon (WSOC) with 4 min integration time over a polluted megacity, New Delhi. Black carbon, carbon monoxide (CO), nitrogen oxides (NOx), and the chemical composition of non-refractory submicron aerosols were also measured in parallel. Diurnal variability in absorption coefficient (0.05 to 65 Mm^{-1}), mass absorption efficiency (0.01 to 3.4 $m^{-2}\ gC^{-1}$) at 365 nm, and absorption angstrom exponent (AAE) of BrC for different wavelength range ($AAE_{300-400}$: 4.2–5.8; $AAE_{400-600}$: 5.5–8.0; and $AAE_{300-600}$: 5.3–7.3) is discussed. BrC chromophores absorbing at any wavelength showed minimum absorption during afternoon hours, suggesting the effects of boundary layer expansion and their photo-sensitive/volatile nature. On certain days, a considerable presence

* Corresponding author.
E-mail address: nrastogi@prl.res.in (N. Rastogi).
[1] Present address: Department of Environmental Studies, University of Delhi, Delhi 110007, India.

https://doi.org/10.1016/j.scitotenv.2021.148589

of BrC absorbing at 490 nm was observed during nighttime that disappears during the daytime. It appeared to be associated with secondary BrC. Observations also infer that BrC species emitted from the biomass and coal burning are more absorbing among all sources. A fraction of BrC is likely associated with trash burning, as inferred from the spectral characteristics of Factor-3 from the PMF analysis of BrC spectra. Such studies are essential in understanding the BrC characteristics and their further utilization in climate models.

1. Introduction

Carbonaceous aerosols are mainly composed of organic carbon (OC) and black carbon (BC). They affect air quality as well as Earth's radiation balance (Feng et al., 2013; Jo et al., 2016; Lack et al., 2012; Laskin et al., 2015). A considerable fraction of organic aerosol (OA) is documented to be water-soluble, which can act as better cloud condensation nuclei and influence climate cooling and the hydrological cycle (Ramanathan, 2001; Singh et al., 2017). On the other hand, BC is considered the second most important human emission in terms of its climate forcing, considering both its absorption capacity and the emissions (Bond et al., 2013; Lack and Cappa, 2010; Laskin et al., 2015). Earlier, BC was the only known light-absorbing carbonaceous species in atmospheric aerosols, and the OC was considered only as scattering species (Jo et al., 2016; Kirchstetter et al., 2004). In recent years, numerous studies showed that a fraction of OC, termed as brown carbon (BrC), can also absorb solar radiation near UV and visible region (Kirchstetter et al., 2004; Ofner et al., 2011). Recent modeling studies estimate that the light absorption by BrC in different areas of the world may be 27–70% of that due to BC absorption (Lin et al., 2014; Moise et al., 2015; Wang et al., 2014). Further, the presence of BC and BrC in cloud droplets or snow could lead to cloud dissipation/evaporation or snow melting (Bond et al., 2013; Hansen et al., 1997; Laskin et al., 2015). Intense ultraviolet light absorption by BrC can induce atmospheric photochemistry and formation of secondary organic aerosols (SOA) by affecting the generation of reactive species (Mok et al., 2016). A recent study estimates primary BrC emissions from biomass burning, and bio-fuel use are globally 3.9 and 3.0 Tg/y, respectively; whereas, secondary BrC is estimated to be ~5.7 Tg/y (Jo et al., 2016).

In order to assess the effects of BrC on air quality and climate, it is inevitable to understand their significant sources and characteristics in different environments. The BrC can be composed of numerous primary and secondary organic species. Primary oxygenated organics such as humic-like substances (HULIS), similar to terrestrial and aquatic humic and fulvic acids, are known primary BrC species contributed by biogenic and biomass burning (BB) emissions (Graber and Rudich, 2005; Hoffer et al., 2005; Lukács et al., 2007; Srinivas and Sarin, 2014; Wang et al., 2017). Water-soluble organic carbon (WSOC) predominantly consists of secondarily formed oxygenated organic aerosol (Ervens et al., 2011; Weber et al., 2007). All or a fraction of WSOC can be light absorbing depending upon its composition. Both fossil fuel burning (FFB) and BB emissions can be significant sources of BrC (or its precursors) in the atmosphere (Hecobian et al., 2010; Hoffer et al., 2005; Laskin et al., 2009; Lukács et al., 2007; Zhang et al., 2011, 2013). Secondary BrC can form from various atmospheric processes such as aqueous-phase reactions in acidic solutions or oxidation of volatile organic compounds (Laskin et al., 2015 and references therein). Sources and characteristics of BrC may vary on a temporal and spatial scale but, this knowledge is sparse in literature (Desyaterik et al., 2013). The optical properties of BrC are strongly affected by its chemical composition, which depends upon different BrC sources and atmospheric processes.

New Delhi, a megacity and the capital of India, is a rapidly growing economy. The city is highly populated (~16.8 million) with a very high population density (11,320 persons per km^2) as per census 2011. It experiences emissions from various anthropogenic sources such as medium and small-scale industries, power plants, and heavy traffic. Wood blocks, coal, and cow-dung cakes burning by the poor people at various places are prevalent in winter for cooking and keeping themselves warm. Further, wintertime stagnant meteorological conditions including temperature inversions trap the emissions that can produce extremely high aerosol concentrations (Guttikunda and Gurjar, 2012). These sources and meteorological conditions make New Delhi an important site for studying the effects of anthropogenic emissions on ambient air quality. To study this in detail, a scientific campaign was carried out involving multiple research groups from India and abroad. A few studies from this campaign reported the sources of trace gases and $PM_{2.5}$, and aerosol oxidative potential (Lalchandani et al., 2021; Puthussery et al., 2020; Rai et al., 2020; Wang et al., 2020; Singh et al., 2021).

The present study mainly focuses on understanding the high time-resolved temporal variability in the optical characteristics of BrC spectra over New Delhi under wintertime meteorological conditions. Further, positive matrix factorization (PMF) analysis was performed on total organic aerosol (OA) composition and water-soluble BrC spectra to identify significant sources of BrC over New Delhi.

2. Experiment

2.1. Site description

Semi-continuous measurements of water-soluble BrC (hereafter termed as BrC) were carried out in Delhi from January 9th to March 3rd 2018. The sampling site was located in the campus of the Indian Institute of Technology Delhi (IITD, 28.54° N, 77.19° E, 216 m above mean sea level) located in South Delhi. Delhi is surrounded by several cities of the National Capital Region (NCR). Meteorological parameters during the study period are presented in Fig. S1. Delhi receives emissions from a wide variety of local anthropogenic sources, including traffic, industries, power plants, brick kilns, bio-fuel burning, etc. (Guttikunda and Calori, 2013; Rai et al., 2020). In addition, long-range regional transport (hundreds of kilometers) of aerosols from upwind regions (e.g., Punjab, Haryana) also contributes to the air pollution of the study region during winter (Fig. S2a, Bikkina et al., 2019). Recent estimates suggest that Delhi is the world's most polluted megacity, and it may become the world's most populated megacity by 2028 (Rai et al., 2021; UN, 2018; World Health Organization, 2018). Further, Fig. S2b depicts that the major wind directions were northwesterly and westerly, and the wind speed was usually <8 m/s during the study period. Wintertime meteorological conditions (calm winds and shallow boundary layer height) favor the accumulation of pollutants over the region.

2.2. Sampling and analysis

2.2.1. Semi-continuous measurements of BrC and WSOC

To measure BrC present in WSOC, most studies use traditional UV–Vis spectrometric technique (Dasari et al., 2019; Hawkins et al., 2016; Kirillova et al., 2014b; Kumar et al., 2018; Laskin et al., 2009; Sareen et al., 2013; Srinivas et al., 2016; Srinivas and Sarin, 2013, 2014; Zhong and Jang, 2011). The present study uses the method adopted from Hecobian et al. (2010) that semi-continuously measures BrC absorption spectra (300-700 nm) and WSOC mass concentration in ambient $PM_{2.5}$ using an assembled system. This sytem (PILS-LWCC-TOC) consists of a particle-into-liquid sampler (PILS, Model ADI 2081, Applicon

Analytical) coupled to portable UV-Vis spectrophotometer with a liquid waveguide capillary cell (LWCC, World Precision Instrument, Sarasota, FL, 2 m path length) and total organic carbon (TOC, Sievers 900 Portable with Turbo, GE Analytical Instruments) analyzer. Details of this setup are given elsewhere (Rastogi et al., 2009; Rastogi et al., 2015; Satish et al., 2017). The BrC and WSOC data were missing from February 16th to February 26th due to technical problems with the PILS-LWCC-TOC system.

The light absorption coefficient at a given wavelength (b_{abs_λ}) was calculated as follows (as described in Hecobian et al., 2010)

$$b_{abs\_\lambda} = (A_\lambda - A_{700}) * \left(\frac{V_l}{V_a * l}\right) * ln\,10 \quad (1)$$

Here A_λ is the absorbance at a given wavelength, A_{700} is the absorbance at 700 nm to account for any baseline drift, V_l is the PILS liquid sample flow rate (0.7 mL min^{-1}) and V_a is air sampling flow rate (16.7 L min^{-1}). The absorbing path length '*l*' is 2 m.

Using b_{abs} (Mm^{-1}) and WSOC (μg m^{-3}), mass absorption efficiency (MAE, m^2 gC^{-1}; hereafter m^2 g^{-1}) of WSOC was calculated as follows:

$$MAE = \frac{b_{abs\_\lambda}}{WSOC} \quad (2)$$

MAE is a key parameter that describes the total light-absorbing ability of all the chromophores present in the aerosol water extract. It is important to note that all WSOC may or may not be BrC, as BrC is a fraction of WSOC that can be anywhere between zero to one. Therefore, the reported MAE of WSOC shall be considered as the lower limit of water-soluble BrC.

2.2.2. Measurements of other chemical species

The chemical composition of atmospheric non-refractory PM_1 was also measured semi-continuously with a High-Resolution Long Time of Flight Aerosol Mass Spectrometer (HR-LToF-AMS, Aerodyne Research Inc., USA) during January–February-2018. Black carbon (BC) concentrations were measured at seven wavelengths using an Aethalometer (AE 33, Magee Scientific) with a 1 min integration time (Drinovec et al., 2015). Carbon monoxide (CO) and nitrogen oxides (NO_X i.e., NO+NO_2) were measured using gas analyzers (Serinus, Ecotech) with a 2 min integration time. In this manuscript, the time series of different species is plotted with the actual time resolution of the measurements. However, hourly average concentrations of species are used when investigating the relationships among them.

3. Results and discussion

3.1. Temporal variability of the measured species

In this work, the absorption coefficient at 365 nm wavelength (b_{abs_365}) is used as proxy for BrC, and those at 300 to 600 nm are used as a proxy of the BrC spectra. The b_{abs} at 365 nm is often used as a measure of water-soluble BrC in ambient aerosols (Hecobian et al., 2010). Temporal trends of b_{abs_365} and WSOC showed a large diurnal as well as day-to-day variability, ranging from 0.05 to 65 Mm^{-1} (avg: 18 ± 12, 1σ), and 1 to 62 μg m^{-3} (avg: 15.7 ± 8.8, 1σ), respectively, during January–February 2018 (Fig. S3). Overall, WSOC and b_{abs_365} both showed a decreasing trend from January (WSOC: 17 ± 9 μg m^{-3}; b_{abs_365}: 19.4 ± 12.1 Mm^{-1}) to February (WSOC: 14 ± 8 μg m^{-3}; b_{abs_365}: 13 ± 8 Mm^{-1}), and their variability suggests a change in both concentrations and the composition of BrC. Their variability in the same (or different) proportion reflects the variability in BrC concentration (or composition) present in WSOC (Satish et al., 2017). This observation can be attributed to several factors such as variability in their sources and/or source strengths, photo-sensitivity, volatility, and meteorological conditions (Hecobian et al., 2010; Satish et al., 2017; Zhang et al., 2011). Effects of meteorological parameters on the concentrations of BrC and WSOC are visible through time series plots of b_{abs_365} and WSOC (Fig. S3), and meteorological parameters (Fig. S1). Lower temperature appears to favor higher BrC and WSOC concentrations and, strong winds and rain adversely affected their concentrations. Lower concentrations of the measured species were observed during rain events that occurred on January 23rd and February 12th (Figs. S1, S3), which cleaned the atmosphere. However, the atmosphere was quickly recharged with substantial concentrations of various chemical species within a few hours after the rain events, indicating local sources were very active.

The WSOC showed a strong correlation with b_{abs_365} (slope = 1.20 ± 0.007, r^2 = 0.72, n = 11,635, Fig. S4), indicating that a significant fraction of WSOC is BrC chromophores, which are absorbing at 365 nm and coming from similar sources, and/or the MAE of BrC from different sources is of similar magnitude. Here (and everywhere in the text), the slopes are given with standard error. This observed relationship is very similar to that observed over Kanpur during winter 2016 using PILS-LWCC-TOC (Satish et al., 2017). The slope represents average MAE excluding intercept value. Further, the MAE_{365} ranged from 0.01 to 3.4 m^{-2} g^{-1} (1.12 ± 0.46) during the study period. The average MAE_{365} value (1.12) is similar to that reported over Kanpur (1.16) (Satish et al., 2017), but higher in comparison to those reported in literature such as 0.60 over South Dekalb-USA (Hecobian et al., 2010), 0.73 over Pasadena-USA (Zhang et al., 2013), 0.75 (daytime) and 1.13 (nighttime) over Patiala-India (Srinivas et al., 2016). However, it was lower in comparison to values documented over Delhi (1.6) (Kirillova et al., 2014a) and Beijing (1.8) (Cheng et al., 2011). These observations suggest that the Indo-Gangetic Plain region (represented by Patiala, Delhi, and Kanpur) has higher abundances and/or higher absorbing capacity of BrC chromophores than those reported over different sites in the USA whereas, lower than that documented over Beijing, China. Substantial variability in MAE (0.01 to 3.4 m^2 g^{-1}) can be attributed to several reasons, such as varying relative abundance of different sources with distinct absorption properties.

In addition to WSOC and BrC, many other species, representing the presence of various sources, were measured in parallel. Temporal variabilities in the concentrations of CO, NOx, BC_{880}, and BC_{370} are presented in Fig. S3, which reflect a large variability in the emissions from different combustion sources over the megacity. Further, the temporal variability in the relative proportion of BC_{370} over BC_{880} suggests the variability of species from biomass burning emissions compared to other sources during the study period (Fig. S3) (Herich et al., 2011; Rastogi et al., 2020; Sandradewi et al., 2008; Singh et al., 2014; Zotter et al., 2017).

Temporal variability in the concentrations of NH_4^+, SO_4^{2-}, NO_3^-, and Cl^-, measured with HR-LToF-AMS, was also significant (Fig. S5). The NH_4^+ and Cl^- were often very high in the early morning hours due to very high ammonium chloride concentrations being high at low temperature and high relative humidity (Fig. S6). High Cl^- concentrations over Delhi were reported in recent studies (Gani et al., 2018; Tobler et al., 2020; Gunthe et al., 2021). The SO_4^{2-} concentration showed the least variability among all the inorganic species, possibly because of their major perennial sources (Thermal Power Plants and industries) in the surrounding region (Singhai et al., 2017). However, the NO_3^- concentration showed a large variability likely due to changes in the favorable meteorological conditions for secondary nitrate formation during the study period (Hennigan et al., 2008; Rastogi et al., 2011).

3.2. Temporal variability in the characteristics of BrC spectra

Fig. 1a and b depicts the temporal variability in BrC spectra and their MAE (for 300 to 600 nm wavelength range). For a given wavelength (λ), the b_{abs_λ} represents the abundance of BrC species absorbing at λ, whereas MAE_λ represents the MAE of the BrC absorbing at λ, which is a fraction of WSOC. This MAE_λ shall be considered as the lower limit of the BrC at λ, as the actual concentration of this BrC (not measured)

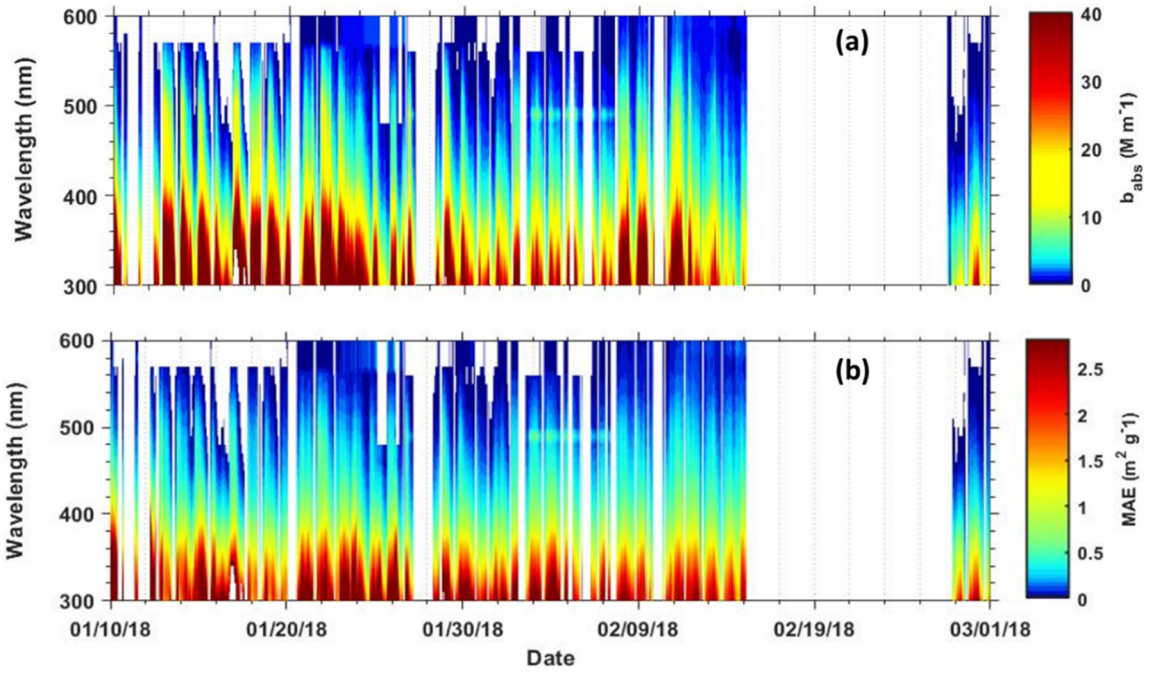

Fig. 1. Temporal variability in (a) BrC spectra and (b) in MAE during the study period.

would be lower than measured WSOC concentration. Further, the variability in the MAEs at different wavelengths reflects the variability in the composition of BrC present in WSOC. As the b_{abs} was measured for 300 to 600 nm, the variability in b_{abs} values and corresponding MAEs was inferred in terms of the variability in the BrC concentration and composition, respectively. To the best of our knowledge, this is a unique measurement hitherto lacking in literature that reveals many interesting features of ambient BrC such as the diurnal and day-to-day variability in the concentrations, composition, and optical characteristics of variety of BrC chromophores absorbing at different wavelengths ranging from 300 to 600 nm. Lin et al. (2016) documented that nitro-aromatics, polyphenols and other benzene-containing chromophores, derivatives of polycyclic aromatic hydrocarbon (PAHs) are present in biomass burning derived aerosols. Further, chromophores in the urban atmosphere often originate from fossil fuel combustion (Lin et al., 2015a, 2015b). Secondary organic aerosols (SOA) formed by the oxidation of volatile organic compounds (VOCs) may also be an important source of atmospheric chromophores. Further, chemical composition and optical properties of the chromophores can be modified through the atmospheric aging processes (Browne et al., 2019; Dasari et al., 2019; Fleming et al., 2020; Kasthuriarachchi et al., 2020; Liu et al., 2016; Romonosky et al., 2019; Satish et al., 2017). In the presence of sunlight or oxidants, photolysis or oxidation can rapidly bleach BrC chromophores by breaking the unsaturated bonds in the molecules and decompose the molecules into colorless carboxylic acids (Hawkins et al., 2016). In this study, it is interesting to note that several chromophores were absorbing not only in near UV wavelength range but also in visible range (Fig. 1a). Several studies showed that primary chromophores (e.g., HULIS) absorb near UV region; whereas, secondary chromophores (e.g., nitro-phenols) usually absorbs in visible region (Hems and Abbatt, 2018; Lin et al., 2015b, 2017; Sun et al., 2007). Abundances of chromophores absorbing in the near UV region were always significant during the study period but, those absorbing in the visible range were often high in January but decreased in February (Fig. 1a). These observations suggest a strong presence of primary BrC source (s) all the time with variable strengths. In the case of secondary BrC, sources of precursors and/or more favorable conditions (higher humidity, lower temperature, calm winds) existed during peak winter (January). However, relatively lower abundances of BrC were observed during February, with further lower concentrations of secondary BrC. Higher abundances were associated with lower temperature and relatively calm winds (Fig. 1a, Fig. S1). The time series plot also shows that there was large variability in BrC composition as well as concentrations. Further, there were several high BrC events in January and a few in February, which are discussed in the subsequent section.

Interestingly, higher or lower BrC concentrations were not necessarily reflected in higher or lower MAE on multiple days (e.g., January 14th, 18th, 19th, 20th, 30th, February 3rd, 4th, 14th, 27th, Fig. 1a, b), suggesting that different BrC species characterized the BrC absorption on different days. The MAE_{λ} doesn't depend upon the b_{abs_λ} alone but on the ratio of b_{abs_λ} to WSOC concentration. During the study period, the MAE showed relatively less variability compared to b_{abs} and WSOC, suggesting that the BrC fraction of WSOC was not as variable as the absolute concentrations.

3.3. Diurnal variability in BrC spectra

BrC is known to be characterized by absorption spectra that smoothly increase from the visible to UV wavelengths. The BrC absorption at different wavelengths is expectedly associated with different chromophores (Laskin et al., 2015 and references therein). The absorption observed at different wavelengths may or may not change uniformly at different times of the day because the atmospheric composition of chromophores may not be uniform all the time (Satish and Rastogi, 2019). Budisulistiorini et al. (2017) showed that the direct burning of several types of biomass could produce primary BrC. Several laboratory studies found that anthropogenic VOCs (such as benzene, toluene, phenols, and polycyclic aromatic hydrocarbons (PAHs)) react with nitrogen oxides and produce light absorbing nitro-aromatics (Moise et al., 2015; Teich et al., 2017). Major sources of primary/secondary BrC could also be different during daytime and nighttime.

Fig. 2 depicts the diurnal variability in BrC spectra, which reveal how hourly average absorption by different chromophores varied within a day during January and February. Abundances of different chromophores would depend upon their primary sources and/or secondary formation processes in the atmosphere. Interestingly, there appears to be various bands of absorption at different wavelengths, which may be due to different groups of BrC species. In January, the highest absorption

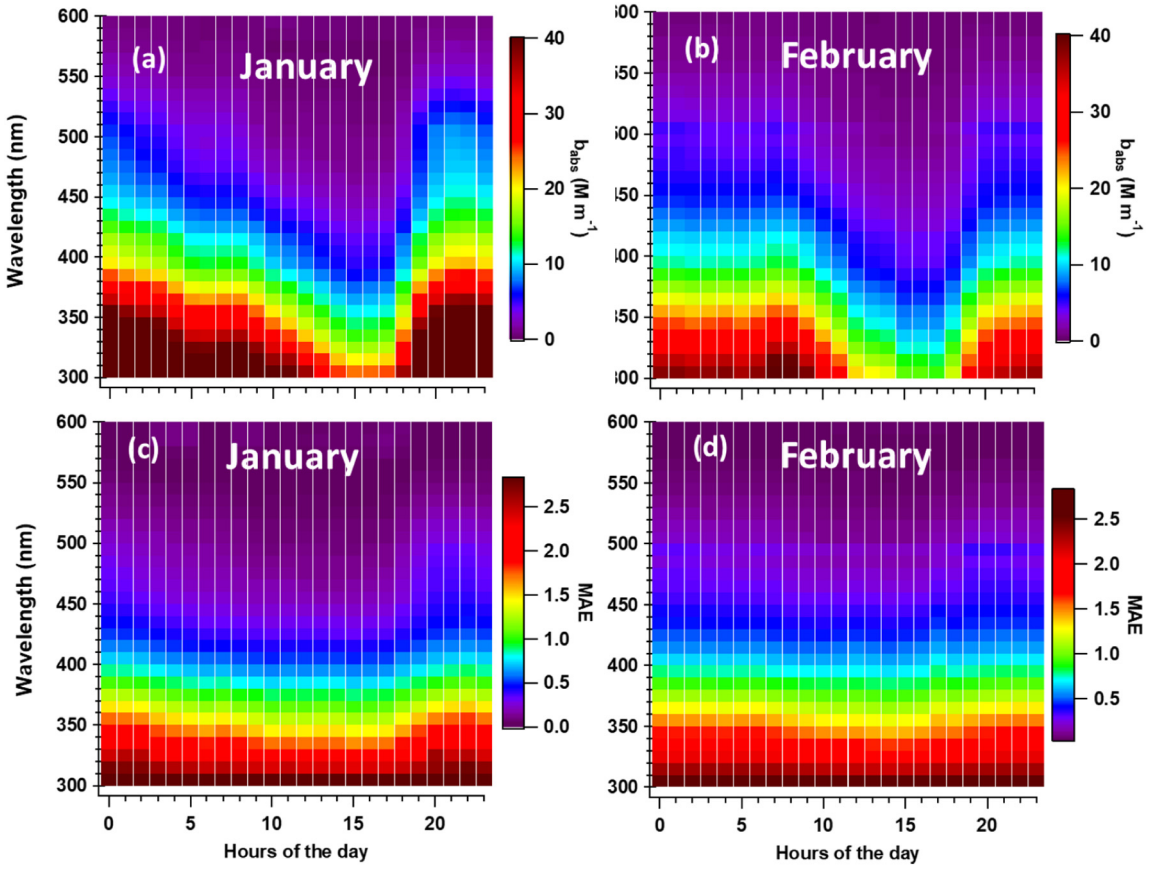

Fig. 2. Diurnal variability in (a) BrC spectra during January and (b) BrC spectra during February, and in (c) MAE during January and (d) MAE during February.

was observed in the 300–360 nm range, followed by 360–390, 390–410, 410–440, 440–460, and 460–530 nm range with a very clear diurnal trend for all the wavelength bands (Fig. 2a). In February, absolute absorption was reduced, and thus, the wavelength band shifted towards lower wavelengths (Fig. 2b); however, the diurnal trends were similar to that observed in January (Fig. 2a). Further, all the BrC chromophores absorbing at any wavelength between 300 and 600 showed minimum absorption during afternoon hours, suggesting the effect of boundary layer expansion (Lalchandani et al., 2021), and/or their photosensitive/volatile nature. Reduction in absolute absorption during day and night from January to February was also observed, indicating that BrC species are likely volatile, as the average temperature was higher in February in comparison to January. This may also be the effect of reduction in certain types of sources e.g., woodblock burning done by poor people to keep themselves and their livestock warm.

MAE showed a noticeable but relatively less diurnal variability compare to b_{abs} (Fig. 2c, d). The b_{abs} represents the abundances of BrC species, whereas MAE represents the relative fraction of BrC in WSOC. Relatively less variability in MAE suggests that the BrC fraction in WSOC and total WSOC both vary in more or less similar fashion; however, nighttime MAE values were significantly higher comparison to daytime MAE values (Fig. 2c, d). This observation suggests the presence of a relatively large BrC fraction in WSOC and/or the presence of relatively more absorbing BrC in WSOC during nighttime. The diurnal differences in MAE were reduced in February compared to January (Fig. 2c, d); however, the absolute MAE values were similar in both months. Variable MAE can be due to multiple reasons such as a difference in the absorption properties of BrC species, change in their abundances under variable meteorological conditions, e.g., through photo-bleaching or volatility. These BrC chromophores can be primary or secondary BrC species from various combustion sources, including BB and FFB emissions. Expanded boundary layer height during daytime can reduce b_{abs} and WSOC values but not MAE, as the MAE is an inherent property of BrC, associated with chemical compositions but not abundances. Diurnal trends of b_{abs} and MAE suggest that secondary BrC formed during daytime are less absorbing, and/or ambient BrC undergoes photobleaching during daytime, and/or they are volatile and evaporates with increasing temperature during daytime (Zhao et al., 2015; Zhong and Jang, 2014). Lalchandani et al. (2021) reported enhanced biomass burning during the night and a larger relative fraction of secondary OA (OOA) during the day for the same site.

3.4. Events with unusually high BrC absorbing in the visible range

A significant absorption peak is observed at around 490 nm during the nighttime of several different days. Fig. 3 depicts snap-shots of the BrC spectra with b_{abs_490} peak observed at 21:30 and/or 03:00 h, and its subsequent change at 09:00, and 16:00 h on a few days of January and February. The b_{abs_490} peak observed on January 21st was very prominent, on February 8th was clearly visible, and that on February 11th was also noticeable. However, the b_{abs_490} peaks on January 21st, February 8th, and February 10th were observed at around 21:30; whereas the one on February 11th was observed at around 03:00. The peak vanished during the daytime. It is understood that the spectral absorbance can be variable at different times of the day if BrC composition is variable. It is well documented that absorption of the visible light is often enhanced in the presence of nitro/nitrate moeties on the molecule, which absorbs strongly in the 400 to 500 nm range (Lin et al., 2015b; Sun et al., 2007). Further, Updyke et al. (2012) reported that secondary organic aerosols change color from white to brown in the presence of ammonia. Browning reaction occurs for a wide range of biogenic and anthropogenic aerosol (Updyke et al., 2012). Based on literature and our observations, it is inferred that the BrC species absorbing at 490 nm are likely nitrogenous organic species. Further, as this peak

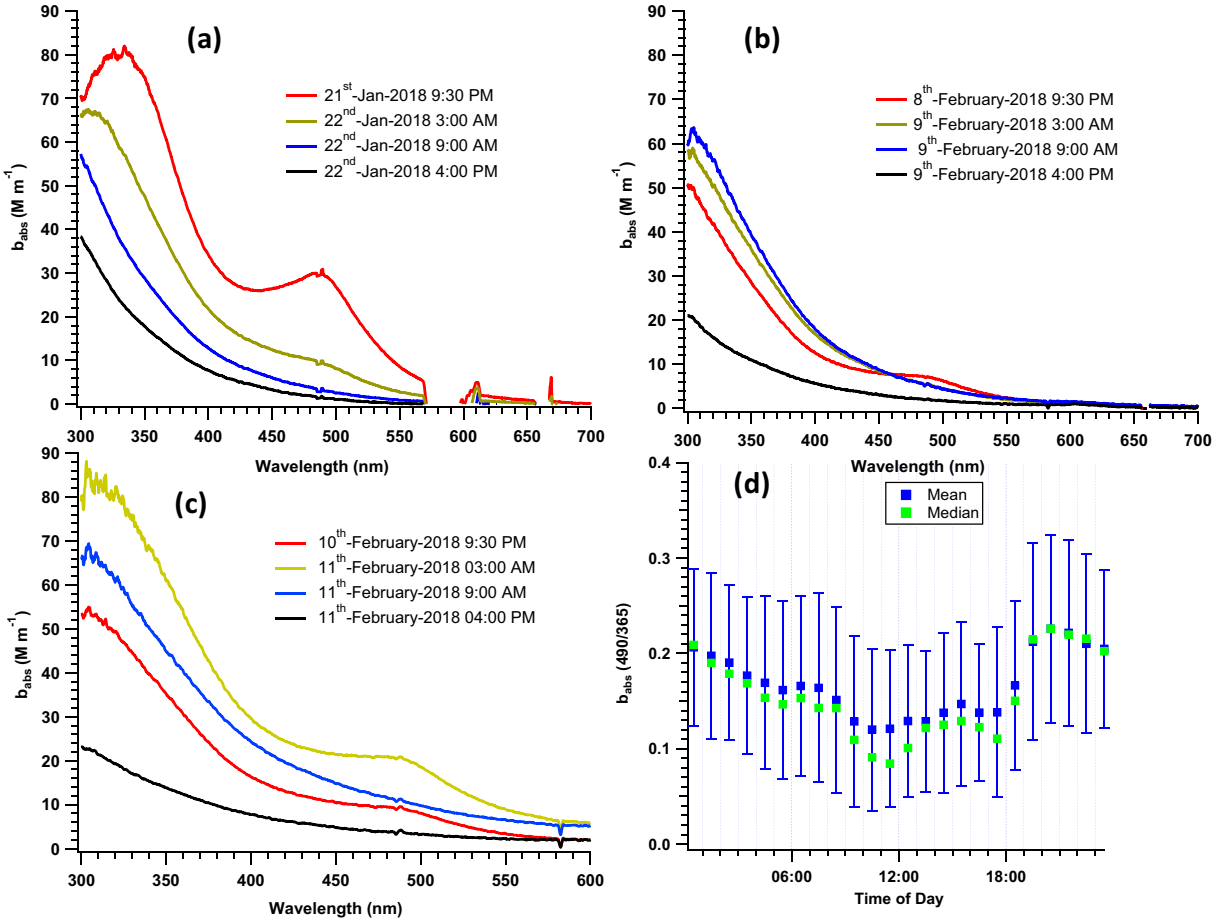

Fig. 3. Spectral variability in BrC on (a) January 21st, (b) February 8th, (c) February 10th and (d) diurnal variability in b_{abs} (490/365) ratio.

disappeared during 09:00 and 16:00 h (daytime) in all the observed events, these BrC species could be likely volatile and/or photo-sensitive.

To investigate this further, the diurnal variability in the ratio of b_{abs_490}/b_{abs_365} is used. Here, the understanding is that if the BrC composition is uniform, the b_{abs} ratio at different wavelengths would remain similar, and if the BrC composition is variable then this ratio would also vary (Satish et al., 2017; Satish and Rastogi, 2019). The absorption ratio of b_{abs_490}/b_{abs_365} exhibited considerable diurnal variability (Fig. 3d), suggesting the presence of BrC_{490} in different amounts at different times. The ratio was minimum during afternoon (14:00 to 17:00), more or less similar during evening and night hours, and exhibit a significant positive hump during 07:00 to 09:00 h and 19:00 to 23:00 h (Fig. 3d), when the traffic emissions are expected to be very high. The hump in b_{abs_490}/b_{abs_365} ratio suggests their fresh formation from the precursors coming from fossil fuel burning. This inference is supported by the diurnal trends of CO and NO_x which were similar to that exhibited by b_{abs_490}/b_{abs_365} ratios (Fig. S7), as the CO and NOx are known proxies of combustion sources. Further, the observed variability could not be due to the changes in boundary layer height because it is expected to affect all the measured species in a similar way, which was not the case.

3.5. Absorption Ångström exponent (AAE)

To assess and explain the spectral characteristics of BC and BrC, Absorption Angström exponent (AAE) is often used in literature. The AAE, representing the wavelength (λ) dependence of BrC absorption, is computed using power law:

$$b_{abs\_\lambda} = K\lambda^{-AAE} \quad (3)$$

where, K is constant and b_{abs_λ} is absorption coefficient of light-absorbing species at a given wavelength (λ) (Arola et al., 2015; Choudhary et al., 2018; Satish et al., 2020; Wu et al., 2016). The AAE reflects the spectral dependence of light absorption from the BrC chromophores present in aqueous solution. The AAE is often used to characterize BrC originating from different sources such as coal combustion, biomass and biofuel burning. Usually, the AAE value of BC is considered as ~1, which is mainly due to liquid fossil-fuel emissions. Furthermore, the AAE value of ~7 is documented for water-soluble humic like substances (HULIS) extracted from aerosols collected in amazon biomass burning plumes, and the values of ~7 to 16 are reported for laboratory-generated smoke from the smoldering of various types of woods (Chen and Bond, 2009; Hoffer et al., 2005). The AAE is also used to investigate the extent of aerosol aging and the underlying formation mechanisms (Browne et al., 2019; Kumar et al., 2018; Liu et al., 2013; Moschos et al., 2018).

In this work, the AAE of BrC is determined from the slope of a linear regression fit between ln (b_{abs_λ}) and ln (λ) for the λ ranging from 300 to 400 nm, 400 to 600 nm, and 300 to 600 nm to understand the AAE of BrC species absorbing in near UV range, visible range, and full range, respectively. Fig. 4a depicts the average b_{abs} spectra during January and February. The light absorption by BrC depicted a sharp increase towards shorter wavelengths in both the months, which is a typical characteristic feature of BrC spectra. The spectral dependence is expected to depend upon the composition of BrC chromophores present in WSOC, and their absorption properties.

Fig. 4b shows the diurnal variability in $AAE_{300-400}$ (range: 4.2 to 5.8, avg. ± sd: 5.1 ± 0.5), $AAE_{400-600}$ (6.1 to 8.0, 7.3 ± 0.5), and $AAE_{300-600}$ (5.9 to 7.3, 6.4 ± 0.4) during January. However, the diurnal variability in $AAE_{300-400}$ (4.5 to 5.0, 4.7 ± 0.1), $AAE_{400-600}$ (5.5 to 6.9, 6.5 ± 0.4), and

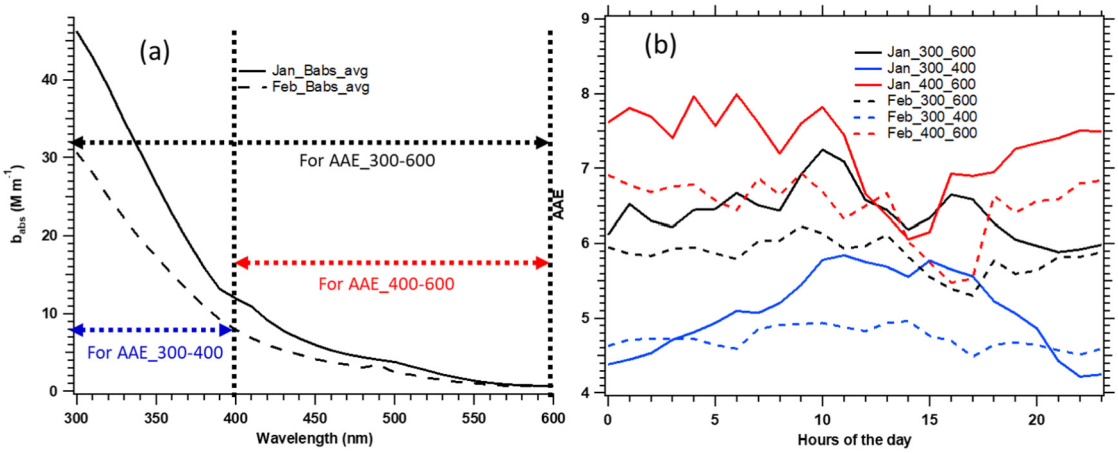

Fig. 4. (a) Average spectral variability of BrC in January and February, and (b) Diurnal variability in AAE for selected wavelength ranges during January and February.

$AAE_{300-600}$ (5.3 to 6.2, 5.8 ± 0.2) during February was noticeably different than that observed during January. These AAE diurnal variabilities mainly reflect the variability in BrC absorption properties. In general, AAE values in a given wavelength range during January were higher than those observed during February for all the three selected wavelength ranges. Observed diurnal trends of AAE can be attributed to the same factors affecting the diurnal trends of b_{abs}. Photo-bleaching/volatile loss of BrC species were likely responsible for higher AAE during afternoon hours, especially for 400–600 and 300–600 wavelength range. AAE for 300–400 range showed relatively less variability, suggesting primary BrC absorbing in this range are least affected photobleaching/volatile loss.

3.6. Sources of BrC chromophores

3.6.1. Relation of BrC with PMF derived OA factors

The chemical composition of non-refractory submicron aerosols was measured with a HR-LToF-AMS. Further, the positive matrix factorization (PMF) analysis was performed on the total organic aerosol (OA) composition. The total OA is represented by six factors, namely hydrocarbon-like OA (HOA), two types of solid-fuel combustion OA (SFCOA-1, SFCOA-2), two types of semi-volatile oxygenated OA (SVOOA-1, SVOOA-2), and a low volatile oxygenated OA (LVOOA) (Fig. S8). The total OA shows a very strong correlation with WSOC measured with PILS-LWCC-TOC system (m = 0.14 ± 0.004, r^2 = 0.79, n = 298, Fig. S9). The observed slope over Delhi is slightly different compared to that reported by Satish et al. (2017) over Kanpur (m = 0.17 ± 0.001, r^2 = 0.79, n = 7380) using a similar experimental setup. A multi regression analysis was performed between OA factors and BrC absorption at different wavelengths to investigate the contribution of specific OA sources to the BrC absorption. Regression parameters (slope and correlation coefficients) of this regression analysis are presented in Table 1. It is clearly shown that the slope values (representing MAE of that factor) decreased exponentially from UV to visible regions for all the factors (Fig. 5). The order of these MAEs were SFCOA-1 > SVOOA-1 > SVOOA-2 > SFCOA-2 > HOA > LVOOA, reflecting the absorption capacity of BrC from these respective source factors (Fig. 5). However, it is important to note that BrC absorption was obtained from water-soluble OA fraction, whereas OA was obtained from the total OA.

The higher slope (MAE) and good regression values were observed at 365 nm for SFCOA-1 (1.01x + 5.35, r^2 = 0.85, n = 536, Table 1), suggesting SFCOA-1 mass is strongly associated with BrC absorption at 365 nm (Alfarra et al., 2007). The MAE values obtained from SFCOOA-1 also showed high absorbing capacity throughout the UV–Visible spectrum compared to the other OA factors (Fig. 5). The SFCOA-1 factor is composed of signals from anhydrous sugars at *m/z* 60 ($C_2H_4O_2$) and *m/z* 73 ($C_3H_5O_2$), which are generally associated with biomass burning (Alfarra et al., 2007). Also, the SFCOA-1 spectra showed the aromatic hydrocarbons peaks like *m/z* 77 (C_6H_5), *m/z* 91 (C_7H_7), and *m/z* 115 (C_9H_7), which may be associated with the coal combustion (Alier et al., 2013; Dall'Osto et al., 2015; Elser et al., 2016). It suggests that the BrC emitted from the BB and coal burning are more absorbing (Lin et al., 2016, 2017; Phillips and Smith, 2014; Satish et al., 2020; Satish and Rastogi, 2019). It is relevant to mention here that coal and wood planks are often used for cooking in slums area of Delhi. Further, SFCOA-1 also showed higher N/C ratios (0.04) and significant amines signals at *m/z* 27 (CHN), *m/z* 30 (CH_4N), *m/z* 41 (C_2H_3N), *m/z* 42 (C_2H_4N), *m/z* 52 (C_3H_2N), *m/z* 54 (C_3H_4N), *m/z* 56 (C_3H_6N) and *m/z* 58 (C_3H_8N), indicating the presence of organic nitrogen (Schneider et al., 2011). Enhanced BrC absorption was also observed in the visible region for MAE of SFCOA-1 (Fig. 5), possibly due to the presence of

Table 1
Regression parameters for linear relationship between BrC absorption coefficient at different wavelengths with OA factors. Slopes indicate the MAE value for individual factors for a given wavelength. The r^2 values in bold font indicate that they were significant at $p < 0.05$.

		365 nm	400 nm	420 nm	450 nm	500 nm	550 nm	600 nm
HOA	Slope + Intercept	0.469x + 9.50	0.252x + 5.30	0.191x + 3.86	0.148x + 2.43	0.106x + 1.22	0.033x + 0.67	0.014x + 0.57
	r2	**0.58**	**0.58**	**0.59**	**0.59**	**0.56**	0.48	0.28
LVOOA	Slope + Intercept	0.191x + 13.18	0.071x + 7.96	0.037x + 6.24	0.016x + 4.53	0.014x + 2.73	0.003x + 1.20	0.0002x + 0.78
	r2	0.044	0.021	0.010	0.004	0.004	0.001	0.000
SFCOA1	Slope + Intercept	1.001x + 5.35	0.528x + 3.23	0.39x + 2.42	0.289x + 1.46	0.198x + 0.65	0.059x + 0.5322	0.035x + 0.45
	r2	**0.85**	**0.81**	**0.78**	**0.72**	**0.63**	0.47	0.31
SFCOA2	Slope + Intercept	0.568x + 8.86	0.299x + 5.05	0.224x + 3.72	0.172x + 2.34	0.123x + 1.16	0.037x + 0.67	0.026x + 0.49
	r2	**0.68**	**0.66**	**0.65**	**0.65**	**0.63**	0.48	0.43
SVOOA1	Slope + Intercept	0.723x + 8.26	0.381x + 4.73	0.284x + 3.49	0.212x + 2.24	0.143x + 1.21	0.040x + 0.75	0.018x + 0.58
	r2	0.31	0.30	0.29	0.28	0.24	0.16	0.06
SVOOA2	Slope + Intercept	0.610x + 8.69	0.297x + 5.31	0.208x + 4.11	0.148x + 2.80	0.107x + 1.53	0.031x + 0.83	0.034x + 0.49
	r2	**0.54**	0.45	0.39	0.33	0.31	0.20	0.13

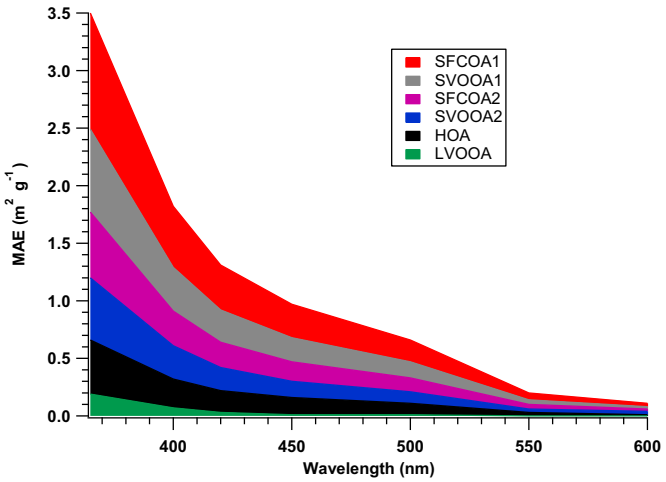

Fig. 5. MAE for different light-absorbing OA components across wavelengths (MAE values are stacked).

nitroaromatics. Further, the lowest MAE values correspond to a very high signal of LVOOA at *m/z* 44 (CO_2^+), and low signals at *m/z* 43 (C_2H_3O), indicating the aged OA oxidized fraction (O/C = 0.49) is less absorbing (Ng et al., 2008; Satish et al., 2017).

3.6.2. PMF analysis of BrC spectra

In addition to the PMF analysis of HR-LToF-AMS derived OA, a PMF analysis on water-soluble BrC spectra was also performed that resulted into a four-factor solution. They represent specific sources of BrC in the observed BrC spectrums. Fig. 6 shows the diurnal variability of these four BrC factors. The first three factors showed substantial diurnal variability with higher concentrations observed during morning rush hour peak between 7 and 10, and an evening peak from 6 pm to 1 am. Further, factor 4 showed an extraordinary trend peaking from 7 am to 4 pm and 5 pm to 1 am, suggesting presence of secondary BrC.

Fig. S10 shows four distinct profiles normalized absorption coefficient across the UV–visible regions. The differences in spectral characteristics from these four factors suggest that BrC came from different emission sources. Factor-1 shows the absorption only in the UV region and peaking at 300 nm. This type of spectrum could due to the presence of nitrate or other inorganic constituents (Hecobian et al., 2010). Factor-2 shows the absorption at both UV and visible regions. It appears like a typical BrC spectrum with higher absorption at UV and gradually reduced absorption values at higher wavelengths. Factor-2 also showed a good correlation with SFCOA-1 and WSOC (Table 2), suggesting that the Factor-2 spectrum is associated with BB or coal-burning emissions. Factor-3 shows a very distinct BrC spectrum. Here, two humps were noticed peaking at 300 nm and 500 nm. The second hump at 500 nm is possibly associated with secondary BrC. A similar type of spectral characteristic was reported by Updyke et al. (2012) for aqueous-phase reactions of limonene SOA formation with ammonia (NH_3) and hydroxyl radical (OH). Further, Factor-3 showed a good correlation with SFCOA-2 ($r^2 = 0.61$, n = 536), which is comprised of saturated hydrocarbons and some oxygenated fragments (*m/z* 27, 41, 55, 69, 71, 83, 85), similar to paper and plastic burning mass spectra reported by (Mohr et al., 2013). This observation suggests that Factor-3 type of spectral characteristics is possibly associated with trash burning. Factor 4 is high during the day in spite of dilution indicating a secondary nature.

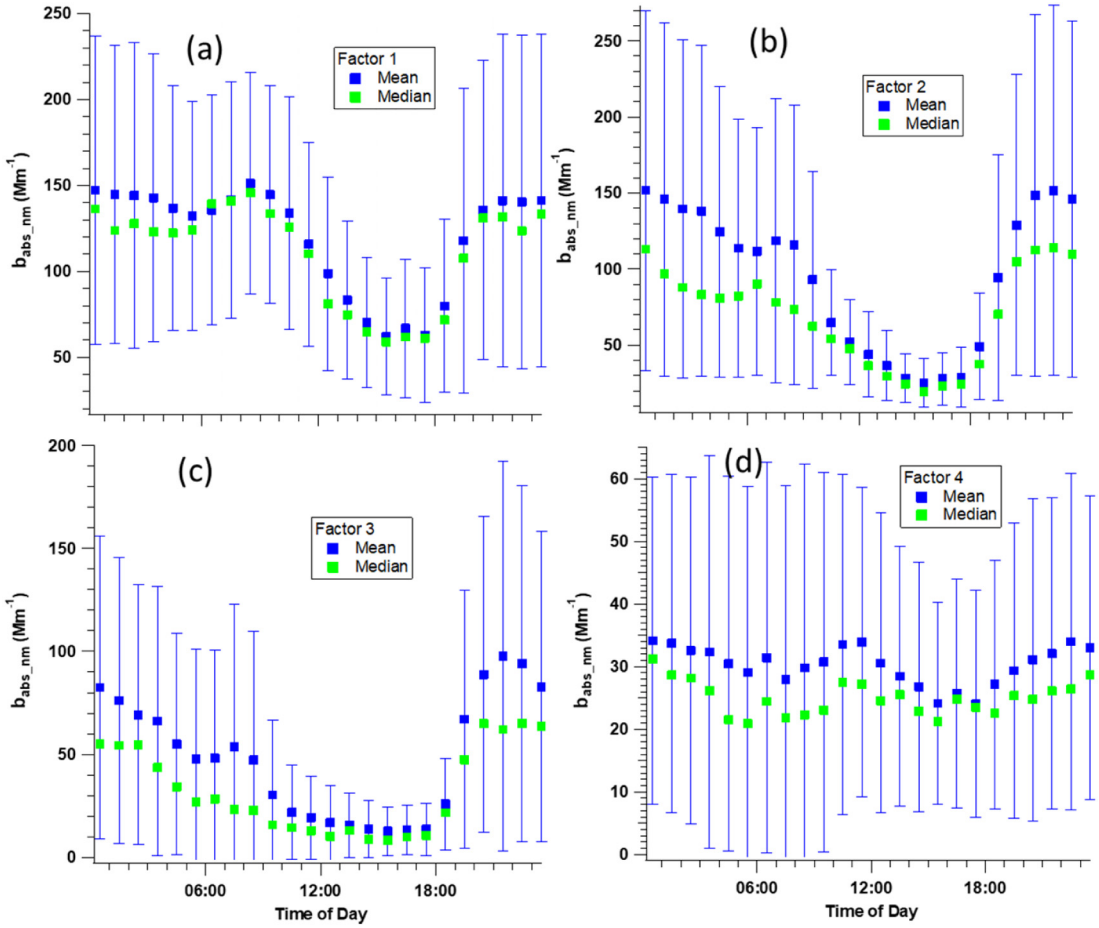

Fig. 6. Diurnal trends of (a) Factor 1, (b) Factor 2, (c) Factor 3, and (d) Factor 4, from the PMF analysis of BrC spectra.

Table 2
Correlation coefficients for linear relationships among PMF derived water-soluble BrC spectra factors and OA factors and WSOC. The r^2 values in bold font indicate that they were significant at $p < 0.05$.

R2	HOA	LVOOA	SFCOA-1	SFCOA-2	SVOOA-1	SVOOA-2	WSOC
Factor-1	0.42	0.09	**0.63**	0.5	0.25	0.57	0.39
Factor-2	0.49	0.07	**0.77**	**0.65**	0.3	**0.65**	**0.67**
Factor-3	**0.57**	–	**0.57**	**0.61**	0.24	0.27	**0.56**
Factor-4	0.11	0.08	0.04	0.04	0.01	0.03	0.04

4. Conclusions

This study reports unique measurements revealing many interesting features of ambient BrC including the diurnal and day-to-day variability in the concentrations and optical characteristics of BrC chromophores absorbing at different wavelengths ranging from 300 to 600 nm over Delhi. Diurnal variability in absorption coefficient, mass absorption efficiency, and absorption angstrom exponent of BrC divulged that the alterations in their characteristics are due to changes in their primary and secondary sources, and meteorological conditions. BrC chromophores absorbing at any wavelength between 300 and 600 nm showed minimum absorption during afternoon hours, suggesting the effects of boundary layer expansion and/or photo-sensitive/volatile nature of BrC chromophores. There was a considerable presence of BrC absorbing at 490 nm during nighttime that disappeared during daytime. On certain days, b_{abs_490} peak was very prominent, and appeared to be associated with secondary BrC. During nighttime, observations indicate the presence of relatively large BrC fraction in WSOC and/or relatively more absorbing BrC in WSOC. PMF analysis of OA and BrC spectra suggest that BrC species emitted from the BB and coal burning are more absorbing among all the sources of BrC. A fraction of BrC may be associated with trash burning, as inferred from the spectral characteristics of Factor-3 from the PMF analysis of BrC spectra. Such studies are very important in comprehensive understanding of the BrC sources and characteristics, and their further utilization in climate models.

CRediT authorship contribution statement

Neeraj Rastogi: Supervision, Resources, Writing – original draft, Writing – review & editing, Project administration. **Rangu Satish:** Methodology, Software, Validation, Formal analysis, Investigation, Writing – review & editing. **Atinderpal Singh:** Methodology, Software, Formal analysis, Investigation, Writing – original draft, Writing – review & editing. **Varun Kumar:** Methodology, Software, Formal analysis, Investigation, Writing – review & editing. **Navaneeth Thamban:** Software, Formal analysis, Investigation, Writing – review & editing. **Vipul Lalchandani:** Methodology, Formal analysis, Investigation, Software, Writing – review & editing. **Ashutosh Shukla:** Methodology, Formal analysis, Investigation, Software, Writing – review & editing. **Pawan Vats:** Writing – review & editing. **S.N. Tripathi:** Writing – review & editing, Project administration, Funding acquisition. **Dilip Ganguly:** Resources, Writing – review & editing. **Jay Slowik:** Investigation, Writing – review & editing. **Andre S.H. Prevot:** Investigation, Writing – review & editing, Project administration, Funding acquisition.

Declaration of competing interest

Authors declare that there is no conflict of interest.

Acknowledgment

SNT gratefully acknowledges the financial support provided by the Department of Biotechnology (DBT), Government of India to conduct this research under grant no. BT/IN/UK/APHH/41/KB/2016-17 dated 19th July 2017 and financial support provided by the Central Pollution Control Board (CPCB). Government of India to conduct this research under grant no. 495 AQM/Source apportionment EPC Project/2017.

Appendix A. Supplementary data

Details on the positive matrix factorization (PMF) analysis of organic aerosols (OA), and Fig S1 to S10 are given in the SI file. Supplementary data to this article can be found online at https://doi.org/10.1016/j.scitotenv.2021.148589.

References

Alfarra, M.R., Prevot, A.S.H., Szidat, S., Sandradewi, J., Lanz, V. a, Schreiber, D., Mohr, M., Baltensperger, U., 2007. Identification of the mass spectral signature of organic aerosols from wood burning emissions identification of the mass spectral signature of organic aerosols from wood burning emissions. Environ. Sci. Technol. 41, 5770–5777. https://doi.org/10.1021/es062289b.

Alier, M., Van Drooge, B.L., Dall'Osto, M., Querol, X., Grimalt, J.O., Tauler, R., 2013. Source apportionment of submicron organic aerosol at an urban background and a road site in Barcelona (Spain) during SAPUSS. Atmos. Chem. Phys. 13, 10353–10371. https://doi.org/10.5194/acp-13-10353-2013.

Arola, A., Schuster, G.L., Pitkänen, M.R.A., Dubovik, O., Kokkola, H., Lindfors, A.V., Mielonen, T., Raatikainen, T., Romakkaniemi, S., Tripathi, S.N., Lihavainen, H., 2015. Direct radiative effect by brown carbon over the Indo-Gangetic Plain. Atmos. Chem. Phys. 15, 12731–12740. https://doi.org/10.5194/acp-15-12731-2015.

Bikkina, S., Andersson, A., Kirillova, E.N., Holmstrand, H., Tiwari, S., Srivastava, A.K., Bisht, D.S., Gustafsson, Ö., 2019. Air quality in megacity Delhi affected by countryside biomass burning. Nat. Sustain. 2, 200–205. https://doi.org/10.1038/s41893-019-0219-0.

Bond, T.C., Doherty, S.J., Fahey, D.W., Forster, P.M., Berntsen, T., Deangelo, B.J., Flanner, M.G., Ghan, S., K??rcher, B., Koch, D., Kinne, S., Kondo, Y., Quinn, P.K., Sarofim, M.C., Schultz, M.G., Schulz, M., Venkataraman, C., Zhang, H., Zhang, S., Bellouin, N., Guttikunda, S.K., Hopke, P.K., Jacobson, M.Z., Kaiser, J.W., Klimont, Z., Lohmann, U., Schwarz, J.P., Shindell, D., Storelvmo, T., Warren, S.G., Zender, C.S., 2013. Bounding the role of black carbon in the climate system: a scientific assessment. J. Geophys. Res. Atmos. 118, 5380–5552. https://doi.org/10.1002/jgrd.50171.

Browne, E.C., Zhang, X., Franklin, J.P., Ridley, K.J., Kirchstetter, T.W., Wilson, K.R., Cappa, C.D., Kroll, J.H., 2019. Effect of heterogeneous oxidative aging on light absorption by biomass burning organic aerosol. Aerosol Sci. Technol. 53, 663–674. https://doi.org/10.1080/02786826.2019.1599321.

Budisulistiorini, S.H., Riva, M., Williams, M., Chen, J., Itoh, M., Surratt, J.D., Kuwata, M., 2017. Light-absorbing brown carbon aerosol constituents from combustion of Indonesian peat and biomass. Environ. Sci. Technol., acs.est.7b00397 https://doi.org/10.1021/acs.est.7b00397.

Chen, Y., Bond, T.C., 2009. Light absorption by organic carbon from wood combustion. Atmos. Chem. Phys. Discuss. 9, 20471–20513. https://doi.org/10.5194/acpd-9-20471-2009.

Cheng, Y., He, K.B., Zheng, M., Duan, F.K., Du, Z.Y., Ma, Y.L., Tan, J.H., Yang, F.M., Liu, J.M., Zhang, X.L., Weber, R.J., Bergin, M.H., Russell, A.G., 2011. Mass absorption efficiency of elemental carbon and water-soluble organic carbon in Beijing, China. Atmos. Chem. Phys. 11, 11497–11510. https://doi.org/10.5194/acp-11-11497-2011.

Choudhary, V., Rajput, P., Singh, D.K., Singh, A.K., Gupta, T., 2018. Light absorption characteristics of brown carbon during foggy and non-foggy episodes over the Indo-Gangetic Plain. Atmos. Pollut. Res. 9, 494–501. https://doi.org/10.1016/j.apr.2017.11.012.

Dall'Osto, M., Paglione, M., Decesari, S., Facchini, M.C., O'Dowd, C., Plass-Duellmer, C., Harrison, R.M., 2015. On the origin of AMS "cooking organic aerosol" at a rural site. Environ. Sci. Technol. 49, 13964–13972. https://doi.org/10.1021/acs.est.5b02922.

Dasari, S., Andersson, A., Bikkina, S., Holmstrand, H., Budhavant, K., Satheesh, S., Asmi, E., Kesti, J., Backman, J., Salam, A., Bisht, D.S., Tiwari, S., Hameed, Z., Gustafsson, Ö., 2019. Photochemical degradation affects the light absorption of water-soluble brown carbon in the South Asian outflow. Sci. Adv. 5, 1–11. https://doi.org/10.1126/sciadv.aau8066.

Desyaterik, Y., Sun, Y., Shen, X., Lee, T., Wang, X., Wang, T., Collett, J.L., 2013. Speciation of "brown" carbon in cloud water impacted by agricultural biomass burning in eastern China. J. Geophys. Res. Atmos. 118, 7389–7399. https://doi.org/10.1002/jgrd.50561.

Drinovec, L., Mocnik, G., Zotter, P., Prevot, A.S.H., Ruckstuhl, C., Coz, E., Rupakheti, M., Sciare, J., Muller, T., Wiedensohler, A., Hansen, A.D.A., 2015. The "dual-spot" Aethalometer: an improved measurement of aerosol black carbon with real-time loading compensation. Atmos. Meas. Tech. 8 (5), 1965–1979. https://doi.org/10.5194/amt-8-1965-2015.

Elser, M., Huang, R., Wolf, R., Slowik, J.G., Wang, Q., Canonaco, F., Li, G., Bozzetti, C., Daellenbach, K.R., Huang, Y., Zhang, R., Li, Z., Cao, J., Baltensperger, U., El-haddad, I., Prévôt, A.S.H., 2016. New Insights Into PM 2.5 Chemical Composition and Sources in Two Major Cities in China During Extreme Haze Events Using Aerosol Mass Spectrometry. , pp. 3207–3225 https://doi.org/10.5194/acp-16-3207-2016.

Ervens, B., Turpin, B.J., Weber, R.J., 2011. Secondary organic aerosol formation in cloud droplets and aqueous particles (aqSOA): a review of laboratory, field and model studies. Atmos. Chem. Phys. 11, 11069–11102. https://doi.org/10.5194/acp-11-11069-2011.

Feng, Y., Ramanathan, V., Kotamarthi, V.R., 2013. Brown carbon: a significant atmospheric absorber of solar radiation. Atmos. Chem. Phys. 13, 8607–8621. https://doi.org/10.5194/acp-13-8607-2013.

Fleming, L.T., Lin, P., Roberts, J.M., Selimovic, V., Yokelson, R., Laskin, J., Laskin, A., Nizkorodov, S.A., 2020. Molecular composition and photochemical lifetimes of brown carbon chromophores in biomass burning organic aerosol. Atmos. Chem. Phys. 20, 1105–1129. https://doi.org/10.5194/acp-20-1105-2020.

Gani, S., Bhandari, S., Seraj, S., Wang, D.S., Patel, K., Soni, P., Arub, Z., Habib, G., Hildebrandt Ruiz, L., Apte, J., 2018. Submicron aerosol composition in the world's most polluted megacity: the Delhi Aerosol Supersite campaign. Atmos. Chem. Phys. Discuss. 5, 1–33. https://doi.org/10.5194/acp-2018-1066.

Graber, E.R., Rudich, Y., 2005. Atmospheric HULIS: how humic-like are they? A comprehensive and critical review. Atmos. Chem. Phys. Discuss. 5, 9801–9860. https://doi.org/10.5194/acpd-5-9801-2005.

Gunthe, S.S., Liu, P., Panda, U., et al., 2021. Enhanced aerosol particle growth sustained by high continental chlorine emission in India. Nat. Geosci. 14, 77–84. https://doi.org/10.1038/s41561-020-00677-x.

Guttikunda, S.K., Calori, G., 2013. A GIS based emissions inventory at 1 km × 1 km spatial resolution for air pollution analysis in Delhi, India. Atmos. Environ. 67, 101–111. https://doi.org/10.1016/j.atmosenv.2012.10.040.

Guttikunda, S.K., Gurjar, B.R., 2012. Role of meteorology in seasonality of air pollution in megacity Delhi, India. Environ. Monit. Assess. 184, 3199–3211. https://doi.org/10.1007/s10661-011-2182-8.

Hansen, J., Sato, M., Ruedy, R., 1997. Radiative forcing and climate response. J. Geophys. Res. Atmos. 102, 6831–6864. https://doi.org/10.1029/96JD03436.

Hawkins, L.N., Lemire, A.N., Galloway, M.M., Corrigan, A.L., Turley, J.J., Espelien, B.M., De Haan, D.O., 2016. Maillard chemistry in clouds and aqueous aerosol as a source of atmospheric humic-like substances. Environ. Sci. Technol. 50, 7443–7452. https://doi.org/10.1021/acs.est.6b00909.

Hecobian, A., Zhang, X., Zheng, M., Frank, N., Edgerton, E.S., Weber, R.J., 2010. Water-soluble organic aerosol material and the light-absorption characteristics of aqueous extracts measured over the Southeastern United States. Atmos. Chem. Phys. 10, 5965–5977. https://doi.org/10.5194/acp-10-5965-2010.

Hems, R.F., Abbatt, J.P.D., 2018. Aqueous phase photo-oxidation of brown carbon nitrophenols: reaction kinetics, mechanism, and evolution of light absorption. ACS Earth Space Chem. 2, 225–234. https://doi.org/10.1021/acsearthspacechem.7b00123.

Hennigan, C.J., Bergin, M.H., Dibb, J.E., Weber, R.J., 2008. Enhanced secondary organic aerosol formation due to water uptake by fine particles. Geophys. Res. Lett. 35, 1–5. https://doi.org/10.1029/2008GL035046.

Herich, H., Hueglin, C., Buchmann, B., 2011. A 2.5 year's source apportionment study of black carbon from wood burning and fossil fuel combustion at urban and rural sites in Switzerland. Atmos. Meas. Tech. 4, 1409–1420. https://doi.org/10.5194/amt-4-1409-2011.

Hoffer, A., Gelencsér, A., Guyon, P., Kiss, G., Schmid, O., Frank, G.P., Artaxo, P., Andreae, M.O., 2005. Optical properties of humic-like substances (HULIS) in biomass-burning aerosols. Atmos. Chem. Phys. Discuss. 5, 7341–7360. https://doi.org/10.5194/acpd-5-7341-2005.

Jo, D.S., Park, R.J., Lee, S., Kim, S.W., Zhang, X., 2016. A global simulation of brown carbon: implications for photochemistry and direct radiative effect. Atmos. Chem. Phys. 16, 3413–3432. https://doi.org/10.5194/acp-16-3413-2016.

Kasthuriarachchi, N.Y., Rivellini, L.H., Adam, M.G., Lee, A.K.Y., 2020. Light absorbing properties of primary and secondary brown carbon in a tropical urban environment. Environ. Sci. Technol. 54, 10808–10819. https://doi.org/10.1021/acs.est.0c02414.

Kirchstetter, T.W., Novakov, T., Hobbs, P.V., 2004. Evidence that the spectral dependence of light absorption by aerosols is affected by organic carbon. J. Geophys. Res. D Atmos. 109, 1–12. https://doi.org/10.1029/2004JD004999.

Kirillova, Elena N., Andersson, A., Tiwari, S., Kumar Srivastava, A., Singh Bisht, D., Gustafsson, Ö., 2014a. Water-soluble organic carbon aerosols during a full New Delhi winter: isotope-base source apportionment and optical properties. J. Geophys. Res. D Atmos. 119, 3476–3485. https://doi.org/10.1002/2013JD021272.Received.

Kirillova, E.N., Marinoni, S.D.A., Bonasoni, P., Facchini, M.C., Fuzzi, S., Vuillermoz, E., 2014b. Light Absorption by Atmospheric Aerosol Brown Carbon in the High Himalayas. vol. 18 p. 40129.

Kumar, N.K., Corbin, J.C., Bruns, E.A., Massabó, D., Slowik, J.G., Drinovec, L., Močnik, G., Prati, P., Vlachou, A., Baltensperger, U., Gysel, M., El-Haddad, I., Prévôt, A.S.H., 2018. Production of particulate brown carbon during atmospheric aging of wood-burning emissions. Atmos. Chem. Phys. Discuss. 1, 1–33. https://doi.org/10.5194/acp-2018-159.

Lack, D.A., Cappa, C.D., 2010. Impact of brown and clear carbon on light absorption enhancement, single scatter albedo and absorption wavelength dependence of black carbon. Atmos. Chem. Phys. 10, 4207–4220. https://doi.org/10.5194/acp-10-4207-2010.

Lack, D.a., Langridge, J.M., Bahreini, R., Cappa, C.D., Middlebrook, a.M., Schwarz, J.P., 2012. Brown carbon and internal mixing in biomass burning particles. Proc. Natl. Acad. Sci. 109, 14802–14807. https://doi.org/10.1073/pnas.1206575109.

Lalchandani, V., Kumar, V., Tobler, A., Thamban, N.M., Mishra, S., Slowik, J.G., Bhattu, D., Rai, P., Satish, R., Ganguly, D., Tiwari, Suresh, Rastogi, N., Tiwari, Shashi, Močnik, G., Prévôt, A.S.H., Tripathi, S.N., 2021. Real-time characterization and source apportionment of fine particulate matter in the Delhi megacity area during late winter. Sci. Total Environ. 770. https://doi.org/10.1016/j.scitotenv.2021.145324.

Laskin, A., Smith, J.S., Laskin, J., 2009. Molecular characterization of nitrogen-containing organic compounds in biomass burning aerosols using high-resolution mass spectrometry. Environ. Sci. Technol. 43, 3764–3771. https://doi.org/10.1021/es803456n.

Laskin, A., Laskin, J., Nizkorodov, S.A., 2015. Chemistry of atmospheric brown carbon. Chem. Rev. 115, 4335–4382. https://doi.org/10.1021/cr5006167.

Lin, G., Penner, J.E., Flanner, M.G., Sillman, S., Xu, L., Zhou, C., 2014. Radiative forcing of organic aerosol in the atmosphere and on snow: effects of SOA and brown carbon. J. Geophys. Res. Atmos. 119, 7453–7476. https://doi.org/10.1002/2013JD021186.

Lin, P., Laskin, J., Nizkorodov, S.A., Laskin, A., 2015a. Revealing brown carbon chromophores produced in reactions of methylglyoxal with ammonium sulfate. Environ. Sci. Technol. 49, 14257–14266. https://doi.org/10.1021/acs.est.5b03608.

Lin, P., Liu, J., Shilling, J.E., Kathmann, S.M., Laskin, J., Laskin, A., 2015b. Molecular characterization of brown carbon (BrC) chromophores in secondary organic aerosol generated from photo-oxidation of toluene. Phys. Chem. Chem. Phys. 17, 23312–23325. https://doi.org/10.1039/C5CP02563J.

Lin, P., Aiona, P.K., Li, Y., Shiraiwa, M., Laskin, J., Nizkorodov, S.A., Laskin, A., 2016. Molecular Characterization of Brown Carbon in Biomass Burning Aerosol Particles. https://doi.org/10.1021/acs.est.6b03024.

Lin, P., Bluvshtein, N., Rudich, Y., Nizkorodov, S.A., Laskin, J., Laskin, A., 2017. Molecular chemistry of atmospheric brown carbon inferred from a nationwide biomass burning event. Environ. Sci. Technol., acs.est.7b02276 https://doi.org/10.1021/acs.est.7b02276.

Liu, J., Bergin, M., Guo, H., King, L., Kotra, N., Edgerton, E., Weber, R.J., 2013. Size-resolved measurements of brown carbon in water and methanol extracts and estimates of their contribution to ambient fine-particle light absorption. Atmos. Chem. Phys. 13, 12389–12404. https://doi.org/10.5194/acp-13-12389-2013.

Liu, J., Lin, P., Laskin, A., Laskin, J., Kathmann, S.M., Wise, M., Caylor, R., Imholt, F., Selimovic, V., Shilling, J.E., 2016. Optical properties and aging of light-absorbing secondary organic aerosol. Atmos. Chem. Phys. 16, 12815–12827. https://doi.org/10.5194/acp-16-12815-2016.

Lukács, H., Gelencsér, A., Hammer, S., Puxbaum, H., Pio, C.A., Legrand, M., Kasper-Giebl, A., Handler, M., Limbeck, A., Simpson, D., Preunkert, S., 2007. Seasonal trends and possible sources of brown carbon based on 2-year aerosol measurements at six sites in Europe. J. Geophys. Res. Atmos. 112, 1–9. https://doi.org/10.1029/2006JD008151.

Mohr, C., Lopez-Hilfiker, F.D., Zotter, P., Prévôt, A.S.H., Xu, L., Ng, N.L., Herndon, S.C., Williams, L.R., Franklin, J.P., Zahniser, M.S., Worsnop, D.R., Knighton, W.B., Aiken, A.C., Gorkowski, K.J., Dubey, M.K., Allan, J.D., Thornton, J.A., 2013. Contribution of nitrated phenols to wood burning brown carbon light absorption in detling, United Kingdom during winter time. Environ. Sci. Technol. 47, 6316–6324. https://doi.org/10.1021/es400683v.

Moise, T., Flores, J.M., Rudich, Y., 2015. Optical properties of secondary organic aerosols and their changes by chemical processes. Chem. Rev. 115, 4400–4439. https://doi.org/10.1021/cr5005259.

Mok, J., Krotkov, N.A., Arola, A., Torres, O., Jethva, H., Andrade, M., Labow, G., Eck, T.F., Li, Z., Dickerson, R.R., Stenchikov, G.L., Osipov, S., Ren, X., 2016. Impacts of brown carbon from biomass burning on surface UV and ozone photochemistry in the Amazon Basin. Sci. Rep. 6, 1–9. https://doi.org/10.1038/srep36940.

Moschos, V., Kumar, N.K., Daellenbach, K.R., Baltensperger, U., Prévôt, A.S.H., El Haddad, I., 2018. Source apportionment of brown carbon absorption by coupling ultraviolet-visible spectroscopy with aerosol mass spectrometry. Environ. Sci. Technol. Lett. 5, 302–308. https://doi.org/10.1021/acs.estlett.8b00118.

Ng, N.L., Kwan, A.J., Surratt, J.D., Chan, A.W.H., Chhabra, P.S., Sorooshian, A., Pye, H.O.T., Crounse, J.D., Wennberg, P.O., Flagan, R.C., Seinfeld, J.H., 2008. Secondary organic aerosol (SOA) formation from reaction of isoprene with nitrate radicals (NO3). Atmos. Chem. Phys. 8, 4117–4140. https://doi.org/10.5194/acp-8-4117-2008.

Ofner, J., Krüger, H.U., Grothe, H., Schmitt-Kopplin, P., Whitmore, K., Zetzsch, C., 2011. Physico-chemical characterization of SOA derived from catechol and guaiacol - a model substance for the aromatic fraction of atmospheric HULIS. Atmos. Chem. Phys. 11, 1–15. https://doi.org/10.5194/acp-11-1-2011.

Phillips, S.M., Smith, G.D., 2014. Light absorption by charge transfer complexes in brown carbon aerosols. Environ. Sci. Technol. Lett. 1, 382–386. https://doi.org/10.1021/ez500263j.

Puthussery, J., Singh, A., Rai, P., Bhattu, D., Kumar, V., Vats, P., Furger, M., Rastogi, N., Slowik, J., Ganguly, D., Prevot, A., Tripathi, S., Verma, V., 2020. Real-time measurements of PM 2.5 oxidative potential using dithiothreitol (DTT) assay in Delhi, India. Environ. Sci. Technol. Lett., XXXX https://doi.org/10.1021/acs.estlett.0c00342.

Rai, P., Furger, M., El Haddad, I., Kumar, V., Wang, L., Singh, A., Dixit, K., Bhattu, D., Petit, J.E., Ganguly, D., Rastogi, N., Baltensperger, U., Tripathi, S.N., Slowik, J.G., Prévôt, A.S.H., 2020. Real-time measurement and source apportionment of elements in Delhi's atmosphere. Sci. Total Environ. 742, 140332. https://doi.org/10.1016/j.scitotenv.2020.140332.

Rai, P., Slowik, J.G., Furger, M., El Haddad, I., Visser, S., Tong, Y., Singh, A., Wehrle, G., Kumar, V., Tobler, A.K., Bhattu, D., Wang, L., Ganguly, D., Rastogi, N., Huang, R.J., Necki, J., Cao, J., Tripathi, S.N., Baltensperger, U., Prevot, A.S.H., 2021. Highly time-resolved measurements of element concentrations in PM10 and PM2.5: comparison of Delhi, Beijing, London, and Krakow. Atmos. Chem. Phys. 21, 717–730. https://doi.org/10.5194/acp-21-717-2021.

Ramanathan, V., 2001. Aerosols, climate, and the hydrological cycle. Science 294, 2119–2124. https://doi.org/10.1126/science.1064034 (80-.).

Rastogi, N., Oakes, M.M., Schauer, J.J., Shafer, M.M., Majestic, B.J., Weber, R.J., 2009. New technique for online measurement of water-soluble Fe(II) in atmospheric aerosols. Environ. Sci. Technol. 43, 2425–2430. https://doi.org/10.1021/es8031902.

Rastogi, N., Zhang, X., Edgerton, E.S., Ingall, E., Weber, R.J., 2011. Filterable water-soluble organic nitrogen in fine particles over the southeastern USA during summer. Atmos. Environ. 45, 6040–6047. https://doi.org/10.1016/j.atmosenv.2011.07.045.

Rastogi, N., Patel, A., Singh, A., Singh, D., 2015. Diurnal variability in secondary organic aerosol formation over the indo-gangetic plain during winter using online measurement of water-soluble organic carbon. Aerosol Air Qual. Res. 15, 2225–2231. https://doi.org/10.4209/aaqr.2015.02.0097.

Rastogi, N., Agnihotri, R., Sawlani, R., Patel, A., Babu, S.S., Satish, R., 2020. Chemical and isotopic characteristics of PM10 over the Bay of Bengal: effects of continental outflow on a marine environment. Sci. Total Environ. 726, 138438. https://doi.org/10.1016/j.scitotenv.2020.138438.

Romonosky, D.E., Gomez, S.L., Lam, J., Carrico, C.M., Aiken, A.C., Chylek, P., Dubey, M.K., 2019. Optical properties of laboratory and ambient biomass burning aerosols: elucidating black, brown, and organic carbon components and mixing regimes. J. Geophys. Res. Atmos. 124, 5088–5105. https://doi.org/10.1029/2018JD029892.

Sandradewi, J., Prévôt, a.S.H., Alfarra, M.R., Szidat, S., Wehrli, M.N., Ruff, M., Weimer, S., Lanz, V.a., Weingartner, E., Perron, N., Caseiro, a., Kasper-Giebl, a., Puxbaum, H., Wacker, L., Baltensperger, U., 2008. Comparison of several wood smoke markers and source apportionment methods for wood burning particulate mass. Atmos. Chem. Phys. Discuss. 8, 8091–8118. https://doi.org/10.5194/acpd-8-8091-2008.

Sareen, N., Moussa, S.G., McNeill, V.F., 2013. Photochemical aging of light-absorbing secondary organic aerosol material. J. Phys. Chem. A 117, 2987–2996. https://doi.org/10.1021/jp309413j.

Satish, R.V., Rastogi, N., 2019. Use of brown carbon spectra as a tool to understand their broader composition and characteristics : a case study from crop residue burning samples. ACS Omega 4, 1847–1853. https://doi.org/10.1021/acsomega.8b02637.

Satish, R.V., Shamjad, P.M., Thamban, N.M., Tripathi, S.N., Rastogi, N., 2017. Temporal characteristics of brown carbon over the Central Indo-Gangetic Plain. Environ. Sci. Technol., acs.est.7b00734 https://doi.org/10.1021/acs.est.7b00734.

Satish, R., Rastogi, N., Singh, A., Singh, D., 2020. Change in Characteristics of Water-soluble and Water-insoluble Brown Carbon Aerosols During a Large-scale Biomass Burning.

Schneider, J., Freutel, F., Zorn, S.R., Chen, Q., Farmer, D.K., Jimenez, J.L., Martin, S.T., Artaxo, P., Wiedensohler, A., Borrmann, S., 2011. Mass-spectrometric identification of primary biological particle markers and application to pristine submicron aerosol measurements in Amazonia. Atmos. Chem. Phys. 11, 11415–11429. https://doi.org/10.5194/acp-11-11415-2011.

Singh, A., Rajput, P., Sharma, D., Sarin, M.M., Singh, D., 2014. Black carbon and elemental carbon from postharvest agricultural-waste burning emissions in the Indo-Gangetic plain. Adv. Meteorol. 2014. https://doi.org/10.1155/2014/179301.

Singh, N., Mhawish, A., Deboudt, K., Singh, R.S., Banerjee, T., 2017. Organic aerosols over Indo-Gangetic Plain: sources, distributions and climatic implications. Atmos. Environ. 157, 59–74. https://doi.org/10.1016/j.atmosenv.2017.03.008.

Singh, A., Rastogi, N., Kumar, V., Slowik, J., Satish, R., Lalchandani, V., Thamban, N., Rai, P., Bhattu, D., Vats, P., Ganguly, D., Tripathi, S.N., Prevot, A.S.H., 2021. Sources and characteristics of light-absorbing fine particulates over Delhi through the synergy of real-time optical and chemical measurements. Atmos. Environ. https://doi.org/10.1016/j.atmosenv.2021.118338.

Singhai, A., Habib, G., Raman, R.S., Gupta, T., 2017. Chemical characterization of PM1.0 aerosol in Delhi and source apportionment using positive matrix factorization. Environ. Sci. Pollut. Res. 24, 445–462. https://doi.org/10.1007/s11356-016-7708-8.

Srinivas, B., Sarin, M.M., 2013. Light absorbing organic aerosols (brown carbon) over the tropical Indian Ocean: impact of biomass burning emissions. Environ. Res. Lett. 8, 044042. https://doi.org/10.1088/1748-9326/8/4/044042.

Srinivas, B., Sarin, M.M., 2014. Brown carbon in atmospheric outflow from the Indo-Gangetic Plain: mass absorption efficiency and temporal variability. Atmos. Environ. 89, 835–843. https://doi.org/10.1016/j.atmosenv.2014.03.030.

Srinivas, B., Rastogi, N., Sarin, M.M., Singh, A., Singh, D., 2016. Mass absorption efficiency of light absorbing organic aerosols from source region of paddy-residue burning emissions in the Indo-Gangetic Plain. Atmos. Environ. 125, 360–370. https://doi.org/10.1016/j.atmosenv.2015.07.017.

Sun, H., Biedermann, L., Bond, T.C., 2007. Color of brown carbon: a model for ultraviolet and visible light absorption by organic carbon aerosol. Geophys. Res. Lett. 34, 1–5. https://doi.org/10.1029/2007GL029797.

Teich, M., Van Pinxteren, D., Wang, M., Kecorius, S., Wang, Z., Müller, T., Močnik, G., Herrmann, H., 2017. Contributions of nitrated aromatic compounds to the light absorption of water-soluble and particulate brown carbon in different atmospheric environments in Germany and China. Atmos. Chem. Phys. 17, 1653–1672. https://doi.org/10.5194/acp-17-1653-2017.

Tobler, A., Bhattu, D., Canonaco, F., Lalchandani, V., Shukla, A., Thamban, N.M., Mishra, S., Srivastava, A.K., Bisht, D.S., Tiwari, S., Singh, S., Močnik, G., Baltensperger, U., Tripathi, S.N., Slowik, J.G., Prévôt, A.S.H., 2020. Chemical characterization of PM(2.5) and source apportionment of organic aerosol in New Delhi, India. Sci. Total Environ. 745, 140924. https://doi.org/10.1016/j.scitotenv.2020.140924.

UN, U.N., 2018. Building health impact assessment in community health promotion. Japanese J. Heal. Educ. Promot. 19, 77–82. https://doi.org/10.11260/kenkokyoiku.19.77.

Updyke, K.M., Nguyen, T.B., Nizkorodov, S.A., 2012. Formation of brown carbon via reactions of ammonia with secondary organic aerosols from biogenic and anthropogenic precursors. Atmos. Environ. 63, 22–31. https://doi.org/10.1016/j.atmosenv.2012.09.012.

Wang, X., Heald, C.L., Ridley, D.A., Schwarz, J.P., Spackman, J.R., Perring, A.E., Coe, H., Liu, D., Clarke, A.D., 2014. Exploiting simultaneous observational constraints on mass and absorption to estimate the global direct radiative forcing of black carbon and brown carbon. Atmos. Chem. Phys. 14, 10989–11010. https://doi.org/10.5194/acp-14-10989-2014.

Wang, Y., Hu, M., Lin, P., Guo, Q., Wu, Z., Li, M., Zeng, Limin, Song, Y., Zeng, Liwu, Wu, Y., Guo, S., Huang, X., He, L., 2017. Molecular characterization of nitrogen-containing organic compounds in humic-like substances emitted from straw residue burning. Environ. Sci. Technol. 51, 5951–5961. https://doi.org/10.1021/acs.est.7b00248.

Wang, L., Slowik, J.G., Tripathi, N., Bhattu, D., Rai, P., Kumar, V., Vats, P., Satish, R., Baltensperger, U., Ganguly, D., Rastogi, N., Sahu, L.K., Tripathi, S.N., Prévôt, A.S.H., 2020. Source characterization of volatile organic compounds measured by proton-transfer-reaction time-of-flight mass spectrometers in Delhi, India. Atmos. Chem. Phys. 20, 9753–9770. https://doi.org/10.5194/acp-20-9753-2020.

Weber, R.J., Sullivan, A.P., Peltier, R.E., Russell, A., Yan, B., Zheng, M., de Grouw, J., Warneke, C., Brock, C., Holloway, J.S., Atlas, E.L., Edgerton, E., 2007. A study of secondary organic aerosol formation in the anthropogenic-influenced southeastern United States. J. Geophys. Res. Atmos. 112, 1–13. https://doi.org/10.1029/2007JD008408.

World Health Organization, 2018. WHO's Ambient (Outdoor) Air Quality Database – Update 2018. pp. 1–4.

Wu, G.M., Cong, Z.Y., Kang, S.C., Kawamura, K., Fu, P.Q., Zhang, Y.L., Wan, X., Gao, S.P., Liu, B., 2016. Brown carbon in the cryosphere: current knowledge and perspective. Adv. Clim. Chang. Res. 7, 82–89. https://doi.org/10.1016/j.accre.2016.06.002.

Zhang, X., Lin, Y.H., Surratt, J.D., Zotter, P., Prevot, A.S.H., Weber, R.J., 2011. Light-absorbing soluble organic aerosol in Los Angeles and Atlanta: a contrast in secondary organic aerosol. Geophys. Res. Lett. 38, 2–5. https://doi.org/10.1029/2011GL049385.

Zhang, X., Lin, Y.H., Surratt, J.D., Weber, R.J., 2013. Sources, composition and absorption Ångström exponent of light-absorbing organic components in aerosol extracts from the Los Angeles Basin. Environ. Sci. Technol. 47, 3685–3693. https://doi.org/10.1021/es305047b.

Zhao, R., Lee, A.K.Y., Huang, L., Li, X., Yang, F., Abbatt, J.P.D., 2015. Photochemical processing of aqueous atmospheric brown carbon. Atmos. Chem. Phys. 15, 6087–6100. https://doi.org/10.5194/acp-15-6087-2015.

Zhong, M., Jang, M., 2011. Light absorption coefficient measurement of SOA using a UV-Visible spectrometer connected with an integrating sphere. Atmos. Environ. 45, 4263–4271. https://doi.org/10.1016/j.atmosenv.2011.04.082.

Zhong, M., Jang, M., 2014. Dynamic light absorption of biomass-burning organic carbon photochemically aged under natural sunlight. Atmos. Chem. Phys. 14, 1517–1525. https://doi.org/10.5194/acp-14-1517-2014.

Zotter, P., Herich, H., Gysel, M., El-Haddad, I., Zhang, Y., Mocnik, G., Hüglin, C., Baltensperger, U., Szidat, S., Prévôt, A.S.H., 2017. Evaluation of the absorption Ångström exponents for traffic and wood burning in the Aethalometer-based source apportionment using radiocarbon measurements of ambient aerosol. Atmos. Chem. Phys. 17, 4229–4249. https://doi.org/10.5194/acp-17-4229-2017.